

Commensurate transverse helical ordering in the room-temperature magnetoelectric Co_2Z hexaferrite

Hun Chang^a, Hak Bong Lee^a, Jae-Ho Chung^{a,*}, Sae Hwan Chun^b, Kwang Woo Shin^b, Byung-Gu Jeon^b, Kee Hoon Kim^b, Karel Prokeš^c, Slavomir Mat'áš^c

^a*Department of Physics, Korea University, Seoul 02841, South Korea*

^b*CeNSCMR, Dept. of Physics and Astronomy, Seoul National University, Seoul 08826, South Korea*

^c*Helmholtz-Zentrum für Materialien und Energie, D-14109 Berlin, Germany*

Abstract

Using single crystal neutron diffraction, we confirmed the existence of the commensurate transverse helical ordering in $\text{Ba}_{0.52}\text{Sr}_{2.48}\text{Co}_2\text{Fe}_{24}\text{O}_{41}$ upon zero-field cooling, in which room-temperature magnetoelectric coupling has been previously observed. Its magnetic structure remained commensurate to the lattice under the external field perpendicular to the c axis. We also found the commensurate ordering to be directly responsible for the electric polarization, which is the common feature of many types of hexaferrites independently of their zero-field orderings.

Keywords: multiferroics, hexaferrites, neutron diffraction, magnetocrystalline anisotropy

1. Introduction

Hexagonal ferrites have long been utilized for industrial applications by virtue of their high Curie temperatures and flexibility encompassing soft to hard ferrimagnetic behaviors.[1] Their high magnetic ordering temperatures are ascribed to strong superexchanges between large spin moments of Fe^{3+} ions ($3d^5, S = 5/2$) built upon the Hund's coupling. In contrast, the hard-

*Corresponding author

Email address: jaehc@korea.ac.kr (Jae-Ho Chung)

ness of a magnet is determined by magnetocrystalline anisotropy fields arising due to unquenched spin-orbit coupling. The layered hexagonal lattices provide highly anisotropic structural symmetry contributing to significant magnetic anisotropy fields. Combinations of these two features in hexaferrites have recently led to the remarkable property observable at room temperature, namely magnetoelectricity.[2] The magnetoelectric couplings, in which electric polarizations appear via magnetic origin, have usually been observed at cryogenic temperatures since magnetic energies are typically weaker than lattice energies.[3, 4, 5, 6, 7] It was only in the hexaferrites where the finite magnetoelectric polarizations have been achieved at room temperature, which also allow both magnetic-field control of electric polarization ($\Delta P - H$) and electric-field control of magnetic polarization ($M - E$).[8, 9, 10]

There are several structural variants of the hexaferrites, in which Fe^{3+} ions occupy crystallographic sites with either four or six oxygen coordinations providing tetrahedral or octahedral crystal fields, respectively.[1] The initial observation of the magnetoelectric polarization was realized in the Y-type $\text{Ba}_{0.5}\text{Sr}_{1.5}\text{Zn}_2\text{Fe}_{12}\text{O}_{22}$ (Zn_2Y) well below room temperature when an external magnetic field was applied perpendicularly to the c axis.[11] Its zero-field magnetic structure is planar helical with incommensurate pitches to the lattice,[12] for which the inverse Dzyalishinskii-Moriya mechanism should not generate finite electric polarizations.[13, 14] Since the planar structure suggests significant easy-plane anisotropy field within ab (or c) planes, fairly strong magnetic field (> 0.2 T) perpendicular to the c axis was required to induce the electric polarization.[11] The magnitude of the onset field could be reduced by more than an order of magnitude upon replacing a few percent of Fe^{3+} ions with Mg^{2+} , Co^{2+} or Al^{3+} ions.[15, 16, 17, 18] The resultant reduction of the easy-plane anisotropy simultaneously caused the magnetic ordering to become heliconical with the net moment along the c axis.[16, 19] Finite magnetoelectric polarizations appear when the helicones tilt off the c axis under the external field.[15, 20] Commonly in different types of hexaferrites, these transverse heliconical orderings are usually found to be commensurate to the structural lattices.[16, 20, 19, 21, 22]

Recently, the room-temperature magnetoelectric coupling was realized in a different type of hexaferrites, namely the Z-type $(\text{Ba,Sr})_3\text{Co}_2\text{Fe}_{24}\text{O}_{41}$ (Co_2Z). [8, 9] Its crystal structure also consists mainly of stacked layers of tetrahedral and octahedral Fe^{3+} sites shared by Co^{2+} ($3d^7$) ions. The high-temperature magnetoelectric coupling is ascribed to magnetic Co^{2+} ($3d^7$) ions contributing to enhancing the electronic exchange strength. As depicted in Fig. 1(a), its structural layers may be grouped into a few blocks, in each of which spin orientations are expected to be internally collinear similarly as in the Y-type. [18] Whereas the smaller S blocks are identical, the larger L block of the Z-type is twice thicker than the counterpart in the Y-type structure. The spiral pitch is driven by the exchange competitions near the L-S interfaces that commonly exist in both types. [23] Contrary to the Y-type, however, the previous study based on neutron powder diffraction suggested that no incommensurate heliconical ordering existed for the Co_2Z in zero field. [24] In this work, we investigated the heliconical magnetic ordering in a single crystal $\text{Ba}_{0.52}\text{Sr}_{2.48}\text{Co}_2\text{Fe}_{24}\text{O}_{41}$, particularly focusing on its existence upon zero-field cooling and the evolution in the transverse magnetic field up to 3 T. We find that the magnetic ordering remained to be commensurate throughout the field range investigated.

2. Experimental

Single crystalline samples were grown using the flux method that is described in Ref. [9]. The largest obtained piece (~ 48 mg) was used for the neutron diffraction measurements while smaller crystals with higher quality were used for magnetoelectric measurements. Commonly in all measurements, crystals were cooled in zero field down to the base temperature and magnetic field was then applied perpendicular to the c axis ($\parallel [\bar{1}20]$). Electric polarization ($\parallel [100]$) was obtained by integrating magnetoelectric current measured following poling simultaneously with $+\mu_0 H_p = 2$ T and $+E = 230$ kV/m.

Single crystal diffraction measurements were performed at the Helmholtz-Zentrum Berlin für Materialien und Energie using the E4 diffractometer ($\lambda =$

2.43 Å). The crystal was oriented with the reciprocal \mathbf{a}^* and \mathbf{c}^* vectors in the horizontal scattering plane before inserting in the superconducting split-pair cryomagnet. Diffraction intensities were collected on the position-sensitive detectors by performing scans in the two-axis mode. The single crystal piece used for neutron diffraction measurements contained three crystallographic domains as well as an Y-type inclusion. While the Bragg reflections from different domains were well separated from each other along $[0\ 0\ l]$ direction, those along $[1\ 0\ l]$ reflections were significantly overlapped. For this reason, we used the two-dimensional Gaussian fitting of the collected data in order to separate their individual intensity contributions.

3. Results and discussions

We searched for the possible presence of incommensurate heliconical magnetic ordering upon zero-field cooling. Since the neutron scattering will have non-zero cross sections only for magnetic moments perpendicular to the momentum transfer, the magnetic intensities due to incommensurate helical ordering within the ab planes will appear along $\mathbf{Q} = l\mathbf{c}^*$ with non-integer values of l . Fig. 2(a) shows the single crystal neutron diffraction intensities observed along the $[0\ 0\ l]$ direction in the reciprocal space during zero-field cooling. From 300 K down to 10 K, we found that all observed peaks appeared only at integer values of l . No evidence was found for the existence of incommensurate peaks, which is a distinct behavior with respect to the magnetoelectric Y- or M-type hexaferrites. At the same time, overall intensities did not show any noticeable changes within the temperature range investigated. The space group symmetry ($P6_3/mmc$) of the Z-type crystal lattice dictates that the structural peaks are forbidden at $00l$ reflections with $l = 2n+1$ ($n = \text{integers}$). The intensities observed at these wave vectors thus should be ascribed entirely to the magnetic ordering of Fe^{3+} spins oriented perpendicular to the c axis. The propagation vector of the associated ordering is $\mathbf{k}_0 = (0,0,1)$, for which spin orientations are reversed between two planes separated by $\frac{1}{2}c$. This separation corresponds, for

instance, to the spacing between the centers of two adjacent L (or S) blocks in Fig. 1(a).

We note that the Bragg peaks observed at $l = 2n$ may also include magnetic intensities as well as structural. The propagation vector of the associated magnetic ordering is $\mathbf{k}_0 = (0,0,0)$, for which spins are oriented parallel between the
100 above-mentioned two planes. Since the magnetic intensities could not be explicitly separated from the structural, instead we observed their intensity changes under the external magnetic field and compared them with the dc magnetization and electric polarization. Fig. 2(b) shows the neutron diffraction intensities at
105 10 K under the external magnetic field that was successively ramped up to 3 T and back down to zero. It is clear that intensities observed at even l values increase under the external field indicating that the \mathbf{k}_0 component develops accordingly. In the meantime, the intensities at odd l values decrease and finally become invisible at 3 T. No intensity was noticed at incommensurate wave
110 vectors under the external field as well. When the external field was ramped back down to zero, the diffraction intensities were recovered for both sets of Bragg peaks. We thus conclude that the magnetic ordering remained to be commensurate to the structure in all temperatures and fields investigated.

In order to have further insights into the magnetic ordering, in Fig. 3 we
115 plotted the integrated intensities of Bragg peaks under the external field. Also plotted are same figure are the dc magnetization (M_{ab}) and electric polarization (ΔP), which were measured along mutually perpendicular directions within the ab planes. Both M_{ab} and ΔP remained very weak at low fields, and simultaneously exhibited sharp increases under the external field. The neutron diffraction
120 intensities, however, remained almost unchanged in the low field range below 0.05 T. (See Figs. 3(c) and 3(d), respectively.) Since it suggests little changes in the underlying magnetic structure, the observed field dependences in this range are primarily ascribed to in-plane rotations of the magnetic domains. The neutron diffraction intensities finally exhibited noticeable changes when
125 the magnetic field exceeded 0.05 T, where a kink is observed also in M_{ab} . The observed changes in this field range indicate that the in-plane \mathbf{k}_0 component of

the magnetic structure increased at the expense of the \mathbf{k}_1 . Simultaneously, the electric polarization approached its maximum value suggesting that the helical component of the magnetic structure became maximized. As the magnetic field was further increase beyond 2 T, both the intensities of $(0\ 0\ 2n)$ reflections and the magnetization finally became saturated whereas those of $(0\ 0\ 2n+1)$ reflections disappeared. We observe that the electric polarization also became zero in this field range indicating that the heliconical magnetic ordering finally collapsed and became collinear [see Fig. 1(b)]. We find that $\Delta P(\mu_B H)$ exhibited a dome-like maximum near 0.2 T, which is distinct from the plateau-like maxima observed in Al-doped Zn_2Y -type.[17] It suggests that the helical component of the Co_2Z experiences relatively weaker pinning force during the field-induced changes near the maximum.

Since the commensurate transverse heliconical ordering must involve magnetic moments along the c axis in addition to those within the ab planes, we expect the \mathbf{k}_1 component to appear also at Bragg reflections with non-zero h indexes. We thus also observe field-dependent changes in the integrated intensity of $(1\ 0\ 0)$ Bragg reflection, which is plotted in Fig. 3(e). Contrary to the case of $(0\ 0\ l)$, this reflection includes contributions both from the \mathbf{k}_0 and \mathbf{k}_1 orderings that cannot be directly separated. Nevertheless, its intensity exhibited a field-induced decrease between 0.05 T and 2.0 T, which provides us with an important clue. Since the \mathbf{k}_0 component must enhance in this range, the apparent decrease in $(1\ 0\ 0)$ intensity should account for the \mathbf{k}_1 component parallel to the c axis. By combining with the zero-field observation, we thus conclude that the transverse conical ordering exists in zero field. The associated magnetic structure is schematically depicted in Fig. 1(b) using the net magnetic moments of L and S spin blocks, or μ_L and μ_S , respectively. While the \mathbf{k}_0 ordering is ascribed to the cone axes perpendicular to the c axis, the \mathbf{k}_1 accounts for the helical component with 90° -itches between neighboring blocks. We suppose that μ_S is more likely to be along the c axis because the S blocks contain more tetrahedral sites.[19] The intensity of the $(1\ 0\ 0)$ reflection eventually was recovered at higher field when the magnetization was saturated, which is consistent

with the \mathbf{k}_0 being maximized. A similar saturation was also observed in the (1 0 1) reflection [see Fig. 3(f).] When the magnetic field was subsequently
160 ramped down to zero, neutron diffraction intensities were almost fully recovered for all reflections as shown in Fig. 3. Although the dc magnetization showed a weak hysteresis, the small remanent magnetization ($0.34 \mu_B/\text{f.u.}$) suggests a weak in-plane coercivity. We do not expect the associated differences to be observable with neutron diffraction.

165 As mentioned previously, the commensurate transverse cones are commonly observed among various types of magnetoelectric hexaferrites. They appear in all magnetoelectric phases of the Y-, M-, and U-types as well as Co_2Z regardless of initial magnetic orderings upon zero-field cooling.[22, 18, 16, 25, 26, 27] Since the structural periods along the c axes are rather long in many hexaferrites,
170 the antiferromagnetic exchanges may not stabilize such commensurate heliconical orderings. For instance, 180° -itches are expected between two ab planes separated by 14.5 \AA for the Y-type, or by 26.1 \AA for the Z-type structures. It has thus been suggested that the two distinct crystal anisotropy fields of the spin blocks play more important roles in locking the commensurate magnetic
175 ordering.[19] What should then be the reason that the transverse conical ordering appears immediately upon zero-field cooling in the Z-type but not in the Y-type? We figure that it is also related to the larger structural period of the Z-type along the c axis. Note that the angles between μ_L and μ_S are determined by the exchange energies across the L-S interfaces as well as two
180 coexisting magnetic anisotropies. The former will primarily affect the in-plane angles whereas those off the planes are determined by the latter.[23] Since the L and S blocks are supposed to possess net easy-plane and easy-axis anisotropy fields, respectively,[19] in the commensurate transverse ordering μ_L should lie within the ab planes while μ_S are tilted off (see Fig. 1). In contrast, both μ_L
185 and μ_S should be off the planes for incommensurate heliconical orderings to appear.[18] All involved spins in this case will have similar tilt angles due to the antiferromagnetic couplings between layers, which is the case for the Y-type upon zero-field cooling.[23, 18] For μ_L to be fixed in the planes while μ_S is not,

however, the tilt angles of the involved spins should gradually increase across
190 the L block towards the L-S interface. We suppose that such arrangement is
achieved in the Z-type because its L block is twice thicker than in the Y-type.
This scenario is also consistent with the commensurate Bragg peaks observed in
the U-type, in which the L block is three times thicker than in the Y-type.[27]

4. Summary and conclusion

195 In summary, we have investigated magnetic ordering of $\text{Ba}_{0.52}\text{Sr}_{2.48}\text{Co}_2\text{Fe}_{24}\text{O}_{41}$
in zero and finite magnetic fields applied perpendicular to the c axis of a single
crystal sample. Magnetic Bragg peaks were observed only at commensurate
wave vectors confirming that the transverse heliconical ordering existed in zero-
field cooling. When the magnetic field was applied, the electric polarization
200 reached its maximum value without significant changes in the underlying mag-
netic structures. The helical ordering finally collapsed at high fields coincidentally
with the suppression of electric polarization. We argue that the thickness of the
L block is an important factor in determining the stability of the commensurate
transverse heliconical ordering in magnetoelectric hexaferrites.

205 Acknowledgement

This research was supported by National R&D Program through the Na-
tional Research Foundation of Korea (NRF) funded by the Ministry of Science,
ICT and Future Planning (grant number: NRF-2017K1A3A7A09016303; NRF-
2016R1D1A1B03934157).

210 References

- [1] J. Smit, H. P. J. Wijn, *Ferrites*, Philips Technical Library, Eindhoven (1959)
Chapter IX. Ferrites with hexagonal.
- [2] S.-W. Cheong, M. Mostovoy, Multiferroics: a magnetic twist for ferroelec-
tricity, *Nature Mater.* 6 (2007) 13–20. doi:10.1038/nmat1804.

- 215 [3] N. Hur, S. Park, P. A. Sharma, J. S. Ahn, S. Guha, S.-W. Cheong, Electric polarization reversal and memory in a multiferroic material induced by magnetic fields, *Nature* 429 (2004) 392–395. doi:10.1038/nature02572.
- [4] G. Lawes, A. B. Harris, T. Kimura, N. Rogado, R. J. Cava, O. E.-W. A. Aharony, T. Yildirim, C. B. M. Kenzelmann, , A. P. Ramirez, Mag-
220 netically driven ferroelectric order in $\text{Ni}_3\text{V}_2\text{O}_8$, *Phys. Rev. Lett.* 95 (2005) 087205. doi:10.1103/PhysRevLett.95.087205.
- [5] M. Kenzelmann, A. B. Harris, S. Jonas, C. Broholm, J. Schefer, S. Kim, C. L. Zhang, S.-W. Cheong, O. P. Vajk, , J. W. Lynn, Magnetic inversion symmetry breaking and ferroelectricity in TbMnO_3 , *Phys. Rev. Lett.* 95
225 (2005) 087206. doi:10.1103/PhysRevLett.95.087206.
- [6] K. Taniguchi, N. Abe, Y. I. T. Takenobu, , T. Arima, Ferroelectric polarization flop in a frustrated magnet MnWO_4 induced by a magnetic field, *Phys. Rev. Lett.* 97 (2006) 097203. doi:10.1103/PhysRevLett.97.097203.
- [7] Y. Yamasaki, S. Miyasaka, Y. Kaneko, J.-P. He, T. Arima, , Y. Tokura,
230 Magnetic reversal of the ferroelectric polarization in a multiferroic spinel oxide, *Phys. Rev. Lett.* 96 (2006) 207204. doi:10.1103/PhysRevLett.96.207204.
- [8] Y. Kitagawa, Y. Hiraoka, T. Honda, T. Ishikura, H. Nakamura, T. Kimura, Low-field magnetoelectric effect at room temperature, *Nature Materials* 9
235 (2010) 797–802. doi:10.1038/nmat2826.
- [9] S. H. Chun, Y. S. Chai, B.-G. Jeon, H. J. Kim, Y. S. Oh, I. Kim, H. Kim, B. J. Jeon, S. Y. Haam, J.-Y. Park, S. H. Lee, J.-H. Chung, J.-H. Park, , K. H. Kim, Electric field control of nonvolatile four-state magnetization at room temperature, *Phys. Rev. Lett.* 108 (2012) 177201. doi:10.1103/
240 PhysRevLett.108.177201.
- [10] J. Wu, Z. Shi, J. Xu, N. Li, Z. Zheng, H. Geng, Z. Xie, L. Zheng, Synthesis

and room temperature four-state memory prototype of $\text{Sr}_3\text{Co}_2\text{Fe}_2\text{O}_{41}$ multiferroics, *Appl. Phys. Lett.* 101 (2012) 122903. doi:10.1063/1.4753973.

- [11] T. Kimura, G. Lawes, A. P. Ramirez, Electric polarization rotation in a hexaferrite with long-wavelength magnetic structures, *Phys. Rev. Lett.* 94 (2005) 137201. doi:10.1103/PhysRevLett.94.137201.
- [12] N. Momozawa, Neutron diffraction study of helimagnet $(\text{Ba}_{1-x}\text{Sr}_x)_2\text{Zn}_2\text{Fe}_{12}\text{O}_{22}$, *J. Phys. Soc. Jpn.* 55 (1986) 4007–4013. doi:10.1143/JPSJ.55.4007.
- [13] H. Katsura, N. Nagaosa, A. V. Balatsky, Spin current and magnetoelectric effect in noncollinear magnets, *Phys. Rev. Lett.* 95 (2005) 057205. doi:10.1103/PhysRevLett.95.057205.
- [14] A. B. Harris, Landau analysis of the symmetry of the magnetic structure and magnetoelectric interaction in multiferroics, *Phys. Rev. B* 76 (2007) 054447. doi:10.1103/PhysRevB.76.054447.
- [15] S. Ishiwata, Y. Taguchi, H. Murakawa, Y. Onose, Y. Tokura, Low-magnetic-field control of electric polarization vector in a helimagnet, *Science* 319 (2008) 1643–1646. doi:10.1126/science.1154507.
- [16] H. B. Lee, S. H. Chun, K. W. Shin, B.-G. Jeon, Y. S. Chai, K. H. Kim, J. Schefer, H. Chang, S.-N. Yun, T.-Y. Joung, J.-H. Chung, Helical magnetic order and field-induced multiferroicity of the Co_2Y -type hexaferrite $\text{Ba}_{0.3}\text{Sr}_{1.7}\text{Co}_2\text{Fe}_{12}\text{O}_{22}$, *Phys. Rev. B* 86 (2012) 094435. doi:10.1103/PhysRevB.86.094435.
- [17] S. H. Chun, Y. S. Chai, Y. S. Oh, D. Jaiswal-Nagar, S. Y. Haam, I. Kim, B. Lee, D. H. Nam, K.-T. Ko, J.-H. Park, J.-H. Chung, K. H. Kim, Realization of giant magnetoelectricity in helimagnets, *Phys. Rev. Lett.* 104 (2010) 037204. doi:10.1103/PhysRevLett.104.037204.
- [18] H. B. Lee, Y.-S. Song, J.-H. Chung, S. H. Chun, Y. S. Chai, K. H. Kim, M. Reehuis, K. Prokeš, S. Mat’áš, Field-induced incommensurate-

- 270 to-commensurate phase transition in the magnetoelectric hexaferrite
 $\text{Ba}_{0.5}\text{Sr}_{1.5}\text{Zn}_2(\text{Fe}_{1-x}\text{Al}_x)_{12}\text{O}_{22}$, Phys. Rev. B 83 (2011) 144425. doi:
10.1103/PhysRevB.83.144425.
- [19] H. Chang, H. B. Lee, Y.-S. Song, J.-H. Chung, S. A. Kim, I. H. Oh,
M. Reehuis, J. Schefer, Al doping effect on magnetic phase transitions
275 of magnetoelectric hexaferrite $\text{Ba}_{0.7}\text{Sr}_{1.3}\text{Zn}_2(\text{Fe}_{1-x}\text{Al}_x)_{12}\text{O}_{22}$, Phys. Rev.
B 85 (2012) 064402. doi:10.1103/PhysRevB.85.064402.
- [20] S. Ishiwata, D. Okuyama, K. Kakurai, M. Nishi, Y. Taguchi, ,
Y. Tokura, Neutron diffraction studies on the multiferroic conical magnet
 $\text{Ba}_2\text{Mg}_2\text{Fe}_{12}\text{O}_{22}$, Phys. Rev. B 81 (2010) 174418. doi:10.1103/PhysRevB.
280 81.174418.
- [21] N. Momozawa, Y. Yamaguch, Field-induced commensurate intermediate
phases in helimagnet $(\text{Ba}_{1-x}\text{Sr}_x)_2\text{Zn}_2\text{Fe}_{12}\text{O}_{22}$ ($x=0.748$), J. Phys. Soc. Jpn.
62 (1993) 1292–1304. doi:10.1143/JPSJ.62.1292.
- [22] H. Sagayama, K. Taniguchi, N. Abe, T. H. Arima, Y. Nishikawa, S. I.
285 Yano, Y. Kousaka, J. Akimitsu, M. Matsuura, K. Hirota, Two distinct
ferroelectric phases in the multiferroic Y -type hexaferrite $\text{Ba}_2\text{Mg}_2\text{Fe}_{12}\text{O}_{22}$,
Phys. Rev. B 80 (2009) 180419(R). doi:10.1103/PhysRevB.80.180419.
- [23] N. Momozawa, Y. Nagao, S. Utsumi, M. Abe, Y. Yamaguchi, Cation dis-
tribution and helimagnetic structure of the $\text{Ba}_2(\text{Zn}_{1-x}\text{Mg}_x)_2\text{Fe}_{12}\text{O}_{22}$ sys-
290 tem as revealed by magnetization measurements and neutron diffraction,
J. Phys. Soc. Jpn. 70 (2001) 2724–2732. doi:10.1143/JPSJ.70.2724.
- [24] M. Soda, T. Ishikura, H. Nakamura, Y. Wakabayashi, T. Kimura, Mag-
netic ordering in relation to the room-temperature magnetoelectric effect
of $\text{Sr}_3\text{Co}_2\text{Fe}_{24}\text{O}_{41}$, Phys. Rev. Lett. 106 (2011) 087201. doi:10.1103/
295 PhysRevLett.106.087201.
- [25] O. P. Aleshko-Ozhevskii, R. A. Sizov, I. I. Yamzin, V. A. Lubimt-

sev, Helicoidal antiphase spin ordering in hexagonal ferrites of the $\text{BaSc}_x\text{Fe}_{12-x}\text{O}_{19}(\text{M})$ system, Soviet Physics JETP 28 (1969) 425.

[26] Y. Tokunaga, Y. Kaneko, D. Okuyama, S. Ishiwata, T. Arima, S. Wakimoto, K. Kakurai, Y. Taguchi, Y. Tokura, Multiferroic *M*-type hexaferrites with a room-temperature conical state and magnetically controllable spin helicity, Phys. Rev. Lett. 105 (2010) 257201. doi:10.1103/PhysRevLett.105.257201.

[27] K. Okumura, T. Ishikura, M. Soda, T. Asaka, H. Nakamura, Y. Wakabayashi, T. Kimura, Magnetism and magnetoelectricity of a U-type hexaferrite $\text{Sr}_4\text{Co}_2\text{Fe}_{36}\text{O}_{60}$, Appl. Phys. Lett. 98 (2011) 212504. doi:10.1063/1.3593371.

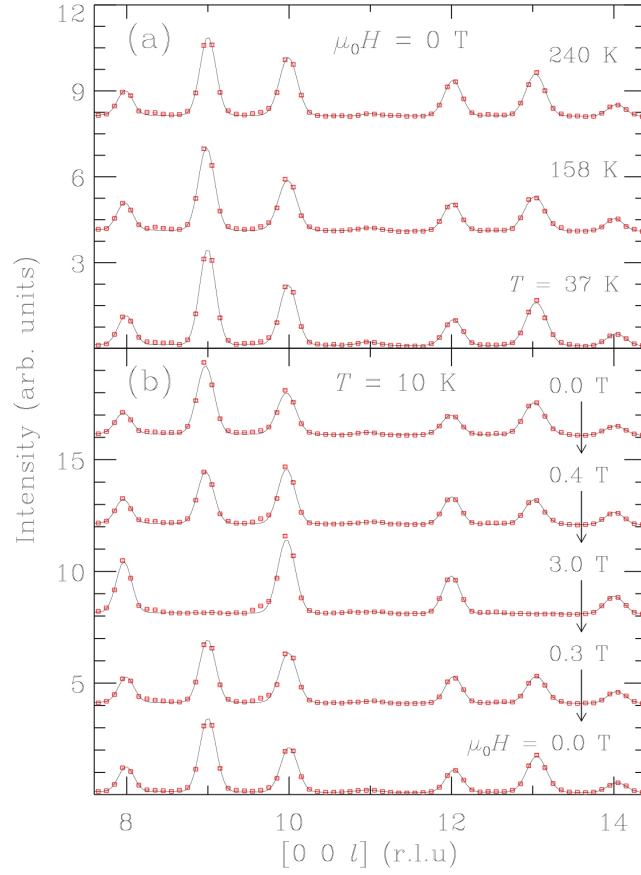


Figure 2: Neutron diffraction intensities observed along the momentum transfer parallel to the c axis (a) at selected temperatures during zero-field cooling or (b) at selected external fields at $T = 10$ K. In (b), the vertical arrow depicts the sequence of measurements during the field ramping up or down.

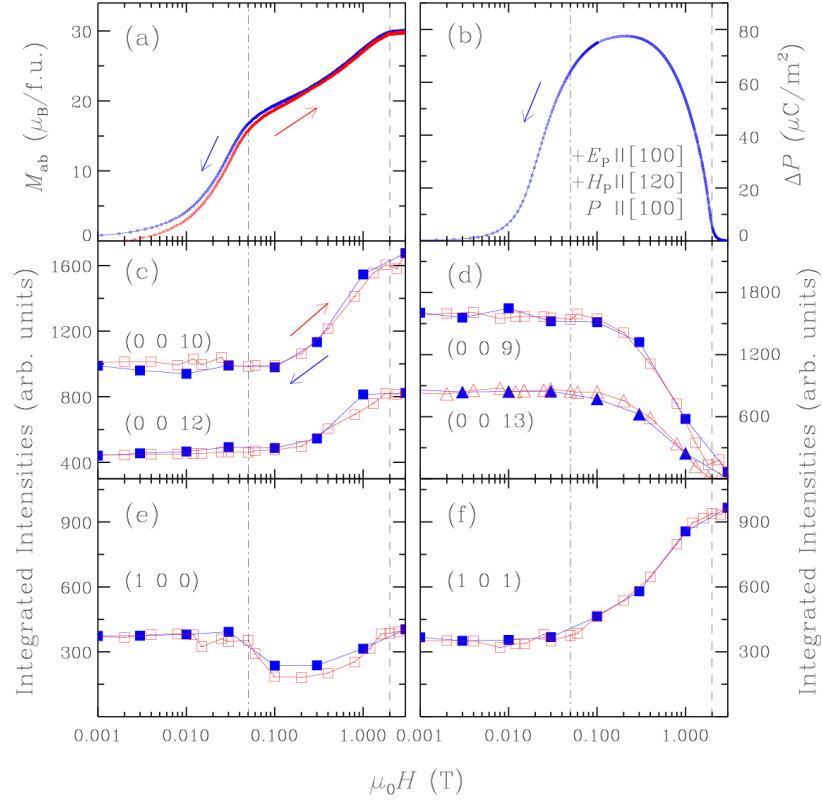


Figure 3: Field-dependent changes at 10 K in (a) dc magnetization, (b) electric polarization, and (c-f) integrated Bragg peak intensities. The arrows indicate the directions of the magnetic field changes during successive measurements. In (c) - (f), the empty and solid symbols represent data measured during ramping up and down, respectively. The dash-dotted and dashed vertical lines mark the field values discussed in the text.